

DE-INTERLEAVED SUBSAMPLING ARCHITECTURE FOR HOMODYNE RECEIVERS

S. A. Bassam, M. Helaoui, and F. M. Ghannouchi

iRadio Lab, Department of Electrical and Computer Engineering
University of Calgary
2500 University Dr. N.W. Calgary, AB, T2N1N4, Canada

Abstract—This paper presents a de-interleaved subsampling receiver architecture suitable for homodyne receivers. The proposed topology requires only a single branch to down-convert and extract the in-phase (I) and quadrature (Q) baseband signals. Using a single-branch receiver eliminates the I/Q mismatch issue of traditional direct down-conversion receivers. The simplicity of the proposed receiver architecture makes it an alternative solution for multi-band and multi-standard applications.

1. INTRODUCTION

In recent years, there have been significant research efforts to design and develop transceivers that are capable of working with different standards in different frequency bands [1, 2]. The idea of multi-standard design was first introduced by Mitola [3], who proposed a receiver topology based on an analog-to-digital converter (ADC) placed right after the antenna to directly digitize the RF signal. However, this simple topology is not yet feasible, mostly due to limitations in designing high-resolution ADCs with high sampling rates of several Gigahertz (GHz). More realistic receiver topologies, such as direct conversion [4], low intermediate frequency (low-IF) [5], and subsampling receivers [6–8] have also been proposed. In the direct conversion receiver, the radio frequency (RF) input signal is directly down-converted to complex baseband signals designated as in-phase (I) and quadrature (Q) signals. In the low-IF architecture, the RF signal is down-converted to intermediate low frequency and directly converted to the digital domain.

In the subsampling technique, the RF signal is down-sampled with a sampling rate much smaller than the RF carrier frequency,

Corresponding author: S. A. Bassam (sabassam@ucalgary.ca).

but at least twice the signal bandwidth. Sampling the RF signal at a rate lower than double rate of the RF will fold the signal to lower frequencies, where these replicates of the RF signal at baseband or IF are used to extract the baseband signal [6–8]. Receivers designed based on this architecture suffer generally from higher noise floors.

An alternative architecture for the subsampling receivers is presented in this work. In [9], we investigated the possibility of using a single-branch receiver to extract the baseband signal. The receiver topology was based on multiplying the RF signal with a square wave, followed by the subsampling technique. This topology was analyzed and validated with measurements. The measurement results were obtained using commercial instruments for low carrier frequencies.

In this paper, a new approach of implementing the de-interleaved subsampling receiver is proposed and validated. With this new approach, a square wave carrier is not needed and is replaced by a single sine wave. This modification reduces the jitter and noise on the LO signal. However, it introduces extra phase distortion to the system, for which a new compensation algorithm is also proposed. This algorithm estimates and compensates for the phase distortion. The proposed architecture is validated with commercial off-the-shelf RF components.

This paper is organized as follows: first, the de-interleaved subsampling receiver architecture is presented. Then, the phase compensation algorithm is explained. Finally, the proposed method is validated with measurements.

2. OVERVIEW OF PREVIOUS TOPOLOGIES

The direct-conversion receiver architecture is the simplest approach to directly down-convert the RF signal to baseband. In this topology, the RF signal is multiplied by in-phase and quadrature LO signals to produce the real part and imaginary parts of the baseband signals respectively, as shown in Fig. 1(a). The simplicity of the topology makes it suitable for integrated circuits; however, impairment issues such as I/Q mismatch, LO leakage and DC (direct current) offsets could considerably degrade the received signal quality [10, 11].

Low-IF architecture [5] is another alternative for frequency down-conversion. As shown in Fig. 1(b), in this topology, the RF signal is first down-converted to a low intermediate frequency; and then, the low-IF signal is directly digitized. In a final step, the down-conversion to baseband and I/Q demodulation are implemented digitally. Therefore, the I/Q mismatch, LO leakage and DC offset issues observed in direct conversion architecture can be avoided. The

major drawback of this topology is the need of a very sharp image rejection filter, since the image signal is very close to the useful signal. Such filter is hard to achieve and integrate when designed in RF frequencies [12, 13].

The last topology, which is reviewed in this paper is based on subsampling technique [6–8, 14]. In this topology, the RF signal is down-sampled with a sampling rate much smaller than the RF carrier frequency. Subsampling the RF signal at a rate lower than the Nyquist rate will produce replicas of the RF signal at lower frequencies. In the subsampling technique one of the replicas at lower frequency is used as an IF signal to extract the baseband I and Q signals. In order to avoid possible aliasing, the sampling rate should be considered according to the following boundaries [8]:

$$\frac{2f_U}{n} \leq f_s \leq \frac{2f_L}{n-1} \text{ where } 1 \leq n \leq \left\lfloor \frac{f_U}{B} \right\rfloor \tag{1}$$

$$f_s \geq 2 \times B \text{ Nyquist rate}$$

where f_L and f_U are the lower and upper frequencies of the band-limited RF signal, $B = f_U - f_L$ is the signal bandwidth, and n is an integer value. Fig. 1(c) shows a receiver topology based on a band-pass sampling technique.

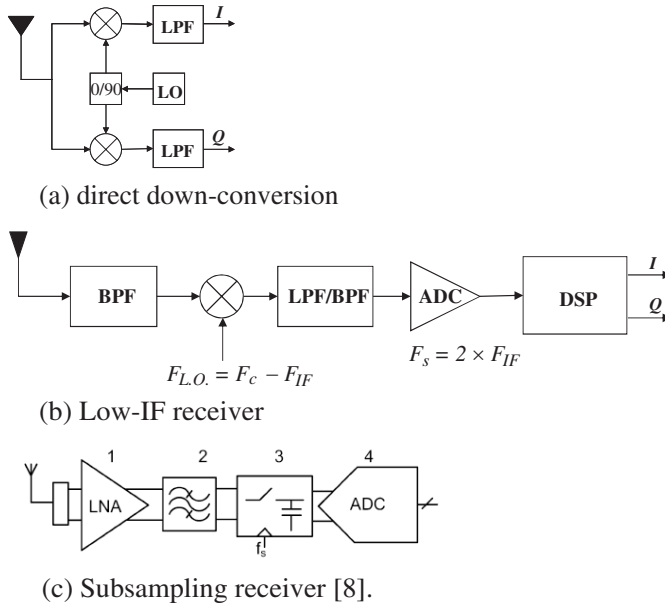


Figure 1. Overview of recent receiver topologies.

In Fig. 1(c), the incoming RF signal is first amplified by a low-noise amplifier (LNA), a sample and hold circuit is used to produce the low-IF replica of the RF signal (based on band-pass sampling technique). Finally, the IF signal is digitized with a high-speed ADC similar to low-IF receiver. This topology is similar to low-IF technique except that the mixer is replaced by a sample and hold circuit. Therefore, similar to a low-IF receiver, this topology suffers from the signal image rejection problem [15].

3. TOPOLOGY OF THE PROPOSED SUBSAMPLING RECEIVER

A block diagram of the proposed receiver topology is depicted in Fig. 2. In this topology, the RF signal is multiplied with a sine wave signal having the same carrier frequency. This results in signals at both the baseband and double the carrier frequency. The subsample version of this signal contains the interleaved version of the baseband I and Q signals. This section describes the proposed topology in detail.

The RF signal with carrier frequency (f_c) can be represented as:

$$V_{RF}(t) = I \cos(\omega_c t + \varphi) - Q \sin(\omega_c t + \varphi) \quad (2)$$

where $\omega_c = 2\pi f_c$, and (φ) represents the phase offset of the transmitter LO relative to the reference. In the following analysis, the phase reference corresponds to the phase of the sampling clock of the ADC. In the first step on the receiver side, the RF signal is multiplied by a sine wave with a frequency equal to the carrier frequency of the signal. The obtained signal is:

$$\begin{aligned} rec(t) &= \{I \cos(\omega_c t + \varphi) - Q \sin(\omega_c t + \varphi)\} \times \sin(\omega_c t + \alpha) \\ &= \frac{I}{2} \{\sin(2\omega_c t + \varphi + \alpha) - \sin(\varphi - \alpha)\} \\ &\quad - \frac{Q}{2} \{\cos(\varphi - \alpha) - \cos(2\omega_c t + \varphi + \alpha)\} \end{aligned} \quad (3)$$

(3) contains terms in both baseband and double the carrier frequency. In (3), (α) and (φ) are the phase offsets of the transmitter and receiver relative to the reference, respectively. Taking into consideration the subsampling rate (F_s) from the following equation:

$$\begin{aligned} T_s &= n \times T_c + \frac{T_c}{4} \text{ where } T_c = \frac{1}{F_c} \\ F_s &= \frac{F_c}{n + \frac{1}{4}} \end{aligned} \quad (4)$$

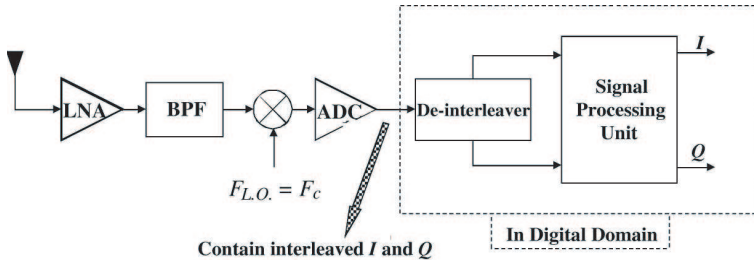


Figure 2. The proposed homodyne subsampling receiver.

From (4), the subsampled version of the received signal ($rec(kT_s)$) is:

$$rec(kT_s) = \frac{I}{2} \{ \sin(k\pi + \varphi + \alpha) - \sin(\varphi - \alpha) \} - \frac{Q}{2} \{ \cos(\varphi - \alpha) - \cos(k\pi + \varphi + \alpha) \} \quad (5)$$

By de-interleaving the signal in (5) to even and odd terms, the result is:

$$\begin{cases} k : even \Rightarrow \begin{cases} rec^{even} = \frac{I}{2} \{ \sin(\varphi + \alpha) - \sin(\varphi - \alpha) \} \\ \quad - \frac{Q}{2} \{ \cos(\varphi - \alpha) - \cos(\varphi + \alpha) \} \end{cases} \\ k : odd \Rightarrow \begin{cases} rec^{odd} = \frac{I}{2} \{ -\sin(\varphi + \alpha) - \sin(\varphi - \alpha) \} \\ \quad - \frac{Q}{2} \{ \cos(\varphi - \alpha) + \cos(\varphi + \alpha) \} \end{cases} \end{cases} \quad (6)$$

where (6) can be written after computation as:

$$\begin{cases} rec^{even} = \{ I \cos(\varphi) - Q \sin(\varphi) \} \times \sin(\alpha) \\ rec^{odd} = \{ I \sin(\varphi) + Q \cos(\varphi) \} \times \cos(\alpha) \end{cases} \quad (7)$$

Looking at (7), there are two phase terms, (α) and (φ), which impact the baseband signal extraction. These two phase terms have different effects on the extracted baseband signals. The phase term, (α), can be seen as the time offset between the LO at the receiver and the sampling clock of the ADC. From (7), it is clear that (α) directly affects the magnitude and phase of the I and Q signals unevenly and leads to gain and phase mismatches. In the design process, the timing between the LO and the ADC sampling clock is adjusted to be $\alpha = \frac{\pi}{4}$. Therefore, the phase term, (α), in such a case, would not affect the baseband signal extraction. The other phase offset term, (φ), is the typical phase offset, and its effect is a phase rotation on the final constellation. It is easily compensated with typical algorithms [16].

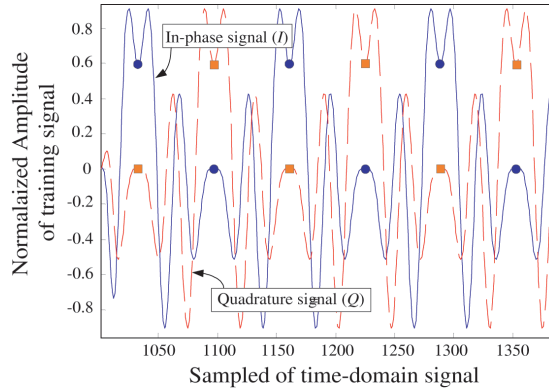


Figure 3. A training sequence used to estimate the phase term (α).

Following the numerical compensation for these two phase offset terms, (α) and (φ), Equation (7) could be simplified as follow:

$$\begin{cases} rec^{even} = I \\ rec^{odd} = Q \end{cases} \quad (8)$$

Equation (8) shows that the de-interleaved signals are represent the in-phase and quadrature baseband signal. Therefore, by subsampling the signal based on (4) and de-interleaved the samples and compensating for the phase offset terms, it is possible to extract the complex baseband signal.

In real implementation, adjusting the exact value of $\alpha = \frac{\pi}{4}$ is not practical, and there is an error in the final product. This error, even as small as it can be, degrades the overall performance of the baseband signal extraction; therefore, it is necessary to estimate the error term and compensate for it digitally at the output of the ADCs. The following compensation algorithm is proposed to compensate for this phase error term. The objective is to develop an algorithm to estimate the offset in (α) using the same training sequences as those for both IEEE 802.11 and 802.16 orthogonal frequency division multiplexing (OFDM) based standards.

Figure 3 shows the I/Q signals of the training sequence. The time steps are marked with circles and squares: when the circle points are non-zeros, the square points are zero, and vice versa. Also, the non-zero values of both the circle and square points have equal values. Taking into account the above properties and using (7), the phase term, (α), can be estimated based on the ratio of the samples at the marked points. Where the estimated phase offset, α_{est} , is proportional to the

tangent of the phase offset (α):

$$\alpha_{est} = \text{atan} \left(\frac{I \cos(\varphi) \sin(\alpha)}{Q \cos(\varphi) \cos(\alpha)} \right) \quad (9)$$

From (8), the phase offset term, (α), can be estimated for any offset away from $\alpha = \frac{\pi}{4}$ and can be easily compensated for afterward. The nominator and denominator in Equation (9) are the non-zero points marked respectively with circle and square in Fig. 3. These non-zeros points have equal magnitude ($I = Q$). Therefore, Equation (9) can be simplified to:

$$\alpha_{est} = \text{atan} \left(\frac{I \cos(\varphi) \sin(\alpha)}{I \cos(\varphi) \cos(\alpha)} \right) = \text{atan} \left(\frac{\sin(\alpha)}{\cos(\alpha)} \right) = \text{atan}(\tan(\alpha)) \quad (10)$$

From (10) and proper selecting the data point from the training sequence, it is possible to estimate the phase offset, (α).

This topology can be easily implemented for multi-standard applications. For that, one need to set the LO frequency equal to the desired carrier frequency and choose a proper subsampling rate based on Equation (4). By adjusting these two parameters the proposed receiver architecture is adjusted for any different standards.

4. SIMULATION AND MEASUREMENT RESULTS

The proposed architecture has been validated with commercial off-the-shelf RF components using an OFDM-based signal with bandwidth equal to 1.25 MHz. The block diagram of the measurement setup is shown in Fig. 4. Two ESG-4438C signal generators, the first used as an RF source and the second as a LO, were used to feed the mixer (MD-141 from M/A-COM, Inc.). The output of the mixer was sampled with an ADC (AD9430), and the sampled data were captured with a high-speed ADC USB FIFO evaluation kit (from analog device). The signal processing was performed in a MATLAB environment.

Using the above measurement setup, the RF signal was mixed with the LO and digitized. The digital signal was de-interleaved and zero padded. The training sequence part of the packet was used first to synchronize the frame and then to estimate and compensate for the error term in the phase offset, (α). The signal-to-noise-distortion ratio (SNDR) was used as the metric in the evaluation of the quality of the received signal compared to the transmitted signal. SNDR is defined as the ratio of the input signal power over the mean power of the difference between the original and received signals. Its expression

is given by:

$$SNDR = 10 \log_{10} \left\langle \frac{\text{mean} \left\{ \sum (I_o^2 + Q_o^2) \right\}}{\text{mean} \left\{ \sum \left\{ (I_o - I_r)^2 + (Q_o - Q_r)^2 \right\} \right\}} \right\rangle \quad (11)$$

where I_o and Q_o are the original in-phase and quadrature baseband signals, respectively; and, I_r and Q_r are the received in-phase and quadrature baseband signals, respectively. The measured SNDR from the above experimental setup was found to be in the vicinity of 20 dB. The actual measured value for the measurement conditions was 18.8 dB.

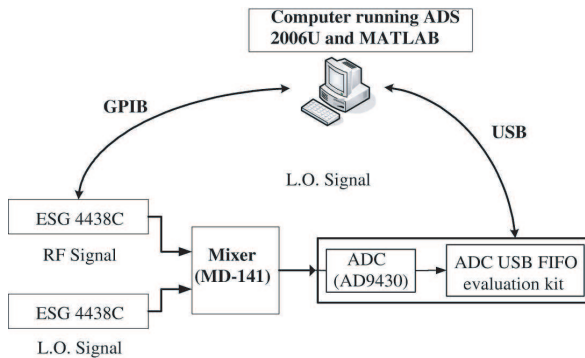


Figure 4. Block diagram of the measurement setup.

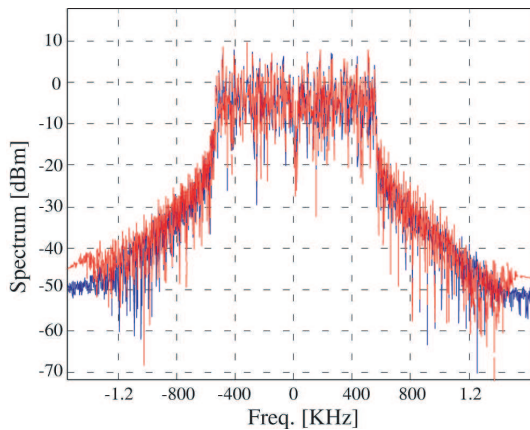


Figure 5. Power spectra of the original (blue solid) and extracted (red dashed) baseband signals.

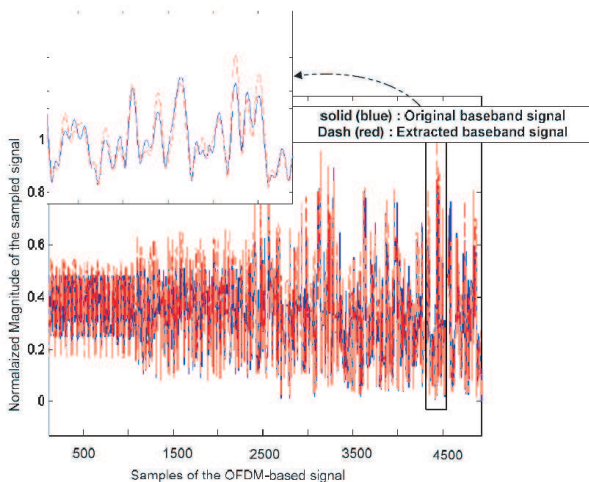


Figure 6. Magnitude of the original and extracted baseband signals.

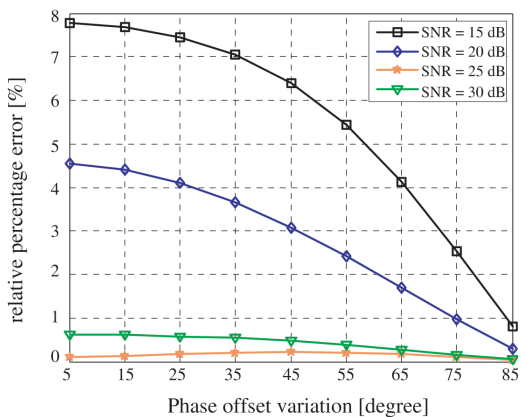


Figure 7. Sensitivity of the phase offset estimation algorithm.

The power spectrum of the original baseband signal and the signal extracted at the output of the new receiver are compared in Fig. 5. A good agreement between both spectra was observed, which proves the soundness and the good performance of the proposed receiver architecture.

In Fig. 6, the magnitude of the original baseband signal and the signal extracted at the receiver output are compared. The results show a good agreement between both time domain envelopes.

The sensitivity of the proposed phase offset estimation and

compensation algorithm over different phase offset values was investigated in MATLAB. For this purpose, a phase offset was intentionally added to the baseband complex signal. Fig. 7 shows the relative percentage error versus the phase offset values for different set of SNRs. The simulation results indicates that the relative percentage error is less than 8% for SNR = 15 dB and eventually it reduced to less than 1% for SNR higher than 25 dB.

5. CONCLUSION

This paper proposed an alternative topology suitable for subsampling receivers based on de-interleaved concepts. The proposed architecture uses a single path to simultaneously down-convert and extract the inphase and quadrature baseband signals. Compared to the available receiver architectures, the proposed topology requires fewer and simpler circuit components. This simplicity makes the proposed receiver a practical solution for low-cost, low-power, multi-standard applications. The proposed receiver topology was tested with an OFDM-based modulated signal. The SNDR of the proposed receiver topology was shown to be better than 18 dB in the measurement results. The sensitivity of the proposed phase offset algorithm over different phase offset values was investigated and it was shown that the relative percentage error on the phase offset estimation would be less than 5% for SNRs higher than 20 dB.

REFERENCES

1. Vidojkovic, M., M. A. T. Sanduleanu, V. Vidojkovic, J. van der Tang, P. Baltus, and A. H. M. van Roermund, "A 1.2 V receiver front-end for multi-standard wireless applications in 65 nm CMOS LP," *34th European Solid-State Circuits Conference, ESSCIRC 2008*, 414–417, Sep. 15–19, 2008.
2. Behjou, N., T. Larsen, and M. Hoegdal, "Design of a simultaneous multi-band RF sub-sampling receiver," *IEEE MTT-S International Microwave Symposium Digest 2008*, 5–8, Jun. 15–20, 2008.
3. Mitola, J., "The software radio architecture," *IEEE Communications Magazine*, Vol. 33, No. 5, 26–38, May 1995.
4. Abidi, A. A., "Direct-conversion radio transceivers for digital communications," *IEEE Journal of Solid-state Circuits*, Vol. 30, No. 12, Dec. 1995.

5. Crols, J. and M. Steyaert, "Low-IF topologies for high-performance analog front-ends for fully integrated receivers," *IEEE Journal of Solid-state Circuits*, Vol. 45, No. 3, Mar. 1998.
6. Vaughan, R. G., N. L. Scott, and D. R. White, "The theorem of bandpass sampling," *IEEE Transactions on Signal Processing*, Vol. 39, 1973–1984, Sep. 1991.
7. Grace, D. and S. P. Pitt, "Quadrature sampling of high frequency waveforms," *Journal of the Acoustical Society of America*, Vol. 44, 1432–1436, 1968.
8. DeVries, C. A. and R. D. Mason, "Subsampling architecture for low power receivers," *IEEE Transactions on Circuits and Systems II: Express Briefs*, Vol. 55, No. 4, Apr. 2008.
9. Bassam, S. A., M. Helaoui, and F. Ghannouchi, "De-interleaved direct down-conversion receiver for SDR applications," *2009 International Microwave Symposium (IMS 2009)*, 1661–1664, Boston, MA, USA, Jun. 7–12, 2009.
10. Razavi, B., "Design considerations for direct conversion receivers," *IEEE Transactions on Circuits and Systems II*, Vol. 44, 428–435, Jun. 1997.
11. Kenington, P. B., *RF and Baseband Techniques for Software Defined Radio*, Artech House, Boston, 2005.
12. Crols, J. and M. Steyaert, *CMOS Wireless Transceiver Design*, Kluwer Academic Publishers, 1997.
13. Fang, S. J., A. Bellaouar, S. T. Lee, and D. J. Allstot, "An image-rejection down-converter for low-IF receivers," *IEEE Transactions on Microwave Theory and Techniques*, Vol. 53, No. 2, 478–487, Feb. 2005.
14. Tseng, C.-H. and S.-C. Chou, "Direct downconversion of multiband RF signals using bandpass sampling," *IEEE Trans. Wireless Communications*, Vol. 5, No. 1, Jan. 2006.
15. Behbahani, F., Y. Kishigami, J. Leete, and A. A. Abidi, "CMOS mixers and polyphase filters for large image rejection," *IEEE Journal of Solid-state Circuits*, Vol. 36, No. 6, 873–887, Jun. 2001.
16. Schmidl, T. M. and D. C. Cox, "Robust frequency and timing synchronization for OFDM," *IEEE Transactions on Communications*, Vol. 45, No. 12, 1613–1621, Dec. 1997.